NUMERICAL STUDY OF SELF AND CONTROLLED INJECTION IN 3-DIMENSIONAL LASER-DRIVEN WAKEFIELDS*

A.W. Davidson, W. Lu, C. Joshi, L.O. Silva, J. Martins, R.A. Foneca, W.B. Mori
UCLA, Los Angeles, CA 90024, USA

Abstract

In plasma based accelerators (LWFA and PWFA), the methods of injecting high quality electron bunches into the accelerating wakefield is of utmost importance for various applications. Understanding how injection occurs in both self and controlled scenarios is therefore important. To simplify this understanding, we start from single particle motion in an arbitrary traveling wave wakefields, an electromagnetic structure with a fixed phase velocity(e.g., wakefields driven by non-evolving drivers), and obtain the general conditions for trapping to occur. We then compare this condition with high fidelity 3D PIC simulations through advanced particle and field tracking diagnostics. Numerous numerical convergence tests were performed to ensure the correctness of the simulations. The agreement between theory and simulations helps to clarify the role played by driver evolution on injection, and a physical picture of injection first proposed[1] is confirmed through simulations. Several ideas, including ionization assisted injection, for achieving high quality controlled injection were also explored and some simulation results relevant to current and future experiments will be presented.

INTRODUCTION

In plasma based accelerators, a wave is induced in a plasma with a phase velocity close to the speed of light[2, 3]. A particle injected in such a wave with sufficient energy will interact with the longitudinal electric field for a long enough time to gain a substantial amount of energy. When a laser pulse is used to induce these wakes, this process is called laser wakefield acceleration (LWFA), whereas when a particle bunch is used it is called plasma wakefield acceleration (PWFA).

For various applications it is important to be able to produce a beam of sufficiently high energy and quality. A simplified understanding of the trapping process may be derived from single particle motion in an arbitrary traveling wave wakefield. The condition for trapping given by this picture is dependent solely on a trapping potential, Ψ, whose evolution may be tracked in our Particle-in-cell (PIC) simulations via a new diagnostic.

A simulation conducted by Lu et al. [1] demonstrated that a monoenergetic bunch of self-injected electrons with energies as high as $1.5GeV$ may be generated by a $200TW$ laser interacting with $0.75cm$ of plasma, having a density of $1.5\times10^{18}cm^{-3}$. This simulation has been repeated with higher order interpolations as well as with a higher particle count in order to assess the accuracy of the original result. Simulations with higher resolution are ongoing.

Ionization-induced injection was also explored. Recent work in both LWFA and PWFA have indicated that, in a partially ionized plasma, electrons may be injected into the wake due to the ionization process induced by the laser or the beam [5]. One method utilizes the large difference in ionization potentials between successive ionization states of trace atoms, for example Nitrogen. For typical parameters the ionized L shell electrons from Nitrogen, and Helium electrons, form the wake, while the electrons from the K shell of Nitrogen, being ionized near the peak of the laser pulse, are injected into the wake. The field of the laser, and not the wake, controls the injection process. This allows the trapping of electrons at both lower plasma densities and lower laser intensities - as is shown in ref. [6]. We have applied our new methods and diagnostics to study the trapping of tunnel ionized electrons, thus further verifying our theoretical understanding of the process.

THEORY

We review a derivation in ref. [7]. A system consisting of a particle with position $\mathbf{x}$ and momentum $\mathbf{P}$ in an arbitrary scalar ϕ and vector $\mathbf{A}$ fields has the Hamiltonian $H = \sqrt{1+|\mathbf{P}-q\mathbf{A}|} + q\phi$, [1] the canonical equations of motion giving

$$\frac{d\mathbf{r}}{dt} = \mathbf{v}, \qquad \frac{d(\mathbf{P}+q\mathbf{A})}{dt} = q(\nabla\mathbf{A}\cdot\mathbf{v} - \nabla\phi). \quad (1)$$

If a field, e.g., ϕ, has the form $\phi(\mathbf{r}_\perp, x - v_\phi t)$, we can show that the time derivative of the Hamiltonian reduces to

$$\frac{dH}{dt} = -qv_\phi\left(\frac{\partial\phi}{\partial x} - \mathbf{v}\cdot\frac{\partial\mathbf{A}}{\partial x}\right). \quad (2)$$

The equations in 1 simplify 2 to $\frac{d}{dt}(H - v_\phi\mathbf{P}) = 0$. Written explicitly as a conserved quantity we obtain the expression

$$\gamma - v_\phi p_x + q(\phi - v_\phi A_x) = Const. \quad (3)$$

From hereon we define the trapping potential $\Psi = \phi - v_\phi A_x$. Ψ is the potential that determines the trapping condition on the particle within a wakefield induced plasma.

Starting from equation 3, we may set the initial and final values for a plasma particle starting at rest ($v_i = 0$) at ψ_i,

* Work supported by the UC Lab Fees Research Award No. 09-LR-05-118764-DOUW, by the US Department of Energy under, DE-FC02-07ER41500 and DE-FG02-92ER40727, and by the National Science Foundation under NSF PHY-0904039 and PHY-0936266. Simulations were done on the Jaguar computer as part of the INCITE award, at NERSC, and on the UCLA Hoffman 2 cluster.

[1] For simplicity, momentum is normalized to mc and energy to mc^2.

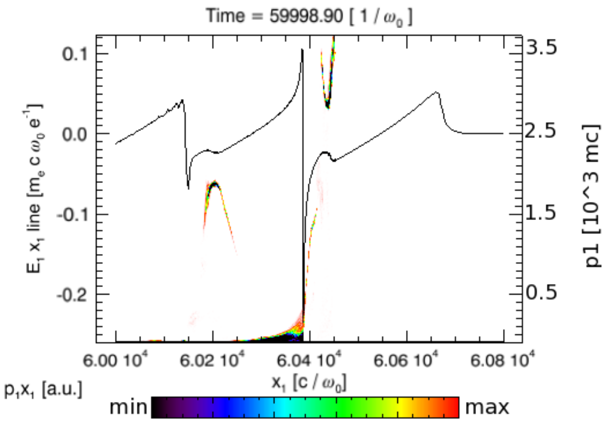

Figure 1: This is the P_x vs x plot superimposed on the lineout of the wakefield, for a quadratic interpolation run with 8 PPC. The effect of the beam loading on the field is greater in both buckets compared to the original run in [1].

and accelerated into the phase velocity of the wake ($v_f = v_\phi$) at trapping potential Ψ_f. This gives us

$$\gamma_f - v_\phi P_\phi - \Psi_f = 1 - \Psi_0,$$

which, solving for the change in the trapping potential ($\Delta\Psi = \Psi_f - \Psi_0$) we obtain the trapping condition for a single particle in arbitrary traveling wakefields[2],

$$\Delta\Psi = \frac{\gamma_f}{\gamma_\phi^2} - 1, \qquad \gamma_f = \sqrt{1 + P_{f\perp}^2}. \tag{4}$$

It should be noted that the canonical momentum is not always conserved in 3D due to a gradient in **A**. However, γ_ϕ is typically high enough that in practice we expect $\Delta\Psi \approx -1$. It is possible to track the evolution of Ψ as a function of time for a particle in a PIC simulation, allowing us to compare our results with this fully explicit picture of particle trapping.

SIMULATIONS

Pre-Ionized Plasma With Self-Injection

In these simulations, as with Lu et al., a circularly polarized $30fs$ (FWHM) $0.8\mu m$ laser pulse containing $200TW$ of power is focused to a spot size $w_0 = 19.5\mu m$ at the entrance of a $1.5 \times 10^{18} cm^{-3}$ density plasma to give a normalized vector potential of $a_0 = 4$.[3] The electrons are then self-injected and accelerated over $7.5mm$ of plasma. The key difference is that we used quadratic, and not linear, interpolation to deposit the current of and the force on the particle on the spatial grid. One additional simulation, with quadratic interpolation, utilized 8 particles-per-grid-cell (PPC) instead of the 2 that was originally used.

[2]This derivation is more thoroughly presented in Wei Lu's Dissertation at UCLA [7].

[3]$a_0 = eA_{\text{laser}}/mc^2$

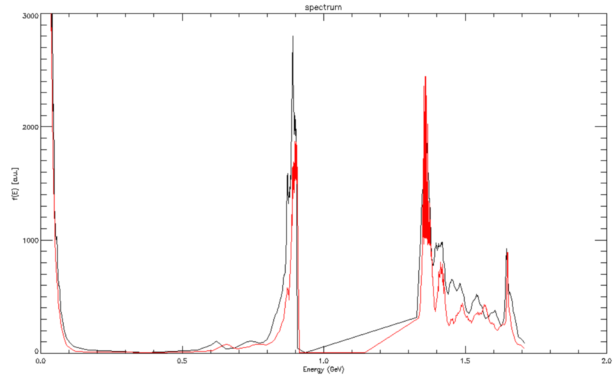

Figure 2: The spectrum of the particles show two monoenergetic beams consistent with ref. [1]. The black line represents a quadratic interpolation with 2 PPC, and the red line represents a quadratic run with 8 PPC.

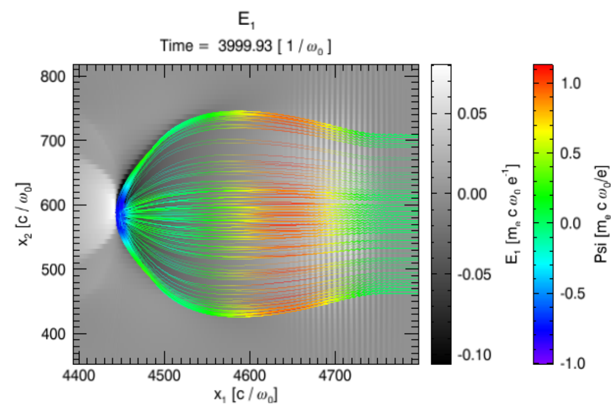

Figure 3: The 2D cross-section of the wake superimposed with the tracks of the particles in the pre-ionized plasma simulation, 0.5 mm into the plasma. Many particles are being injected far from the axis - leading to a greater transverse momentum and lower beam quality. The trapped particles undrego $\Delta\Psi \approx -1$. The tracks that appear to be along the axis are curved towards and away from the viewer.

This simulation produced two monoenergetic bunches which are visible in Figures 1 and 2. Table 1 lists the charge and emittance of the electron bunches trapped in the first and second buckets. The emittance is worse for the higher-order runs, but more notable is the fact that, in addition, three times the amount of charge is trapped in the second bucket. This additional charge causes a greater beam loading, which is visible in Figure 1.

Ionization-Induced Injection

We also simulated a linearly polarized, $60fs$ (FWHM) $0.8\mu m$ laser pulse containing $40TW$ of power focused to a spot size $w_0 = 15.0\mu m$ one millimeter inside a plasma of density $3 \times 10^{18} cm^{-3}$. The electrons were accelerated over a distance of $2.6mm$. The pre-ionized gas contains 99.5%

Table 1: Emittance and Charge trapped in Buckets 1 and 2. Run #1 is the original Lu et al. run, with linear interpolation and 2 particle per cell. Run #2 used quadratic interpolation instead, and #3 used quadratic interpolation and 8 particles per cell.

Run #	$\epsilon_{1,x}$ (π mm rad)	$\epsilon_{1,y}$	q_1 (pC)	$\epsilon_{2,x}$	$\epsilon_{2,y}$	q_2
1	35	29	300	10	11	50
2	42	41	337	25	17	155
3	46	38	344	27	18	150

He and 0.5% N.

This created a beam of $425MeV$ containing $880pC$ of charge, shown in Figure 5. The ionization injection process is nicely shown in the field-tracking diagnostic in Figure 6. Unlike the self-injected case the particles are injected at a high potential, and therefore match equation 4 in a shallower well.

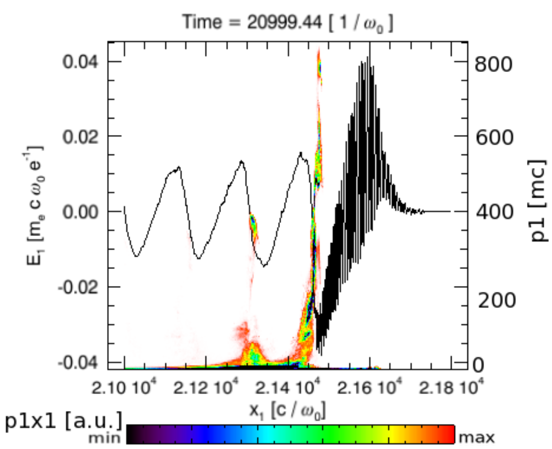

Figure 4: P_x vs x of the $N = 6, 7$ electrons of N, superimposed with the lineout of the wake, after the laser has traversed $2.6mm$ of plasma. The spectrum is in Figure 5.

CONCLUSION

Higher-order and higher-particle-count PIC simulations confirm the results presented in ref. [1]. These were in great agreement with the original, but three times the amount of charge was trapped in the second bucket. In addition, the field and particle tracking diagnostics allowed us to verify our theory of the trapping condition in an arbitrary wake.

The ionization run provided an opportunity to study the trapping of particles under a new method. The field diagnostics show that the ionization-injected particles are able to trap in smaller potential wells, being initially injected at a high potential. In addition, the particles are injected closer to the axis - a property which may be used to produce low emittance beams.

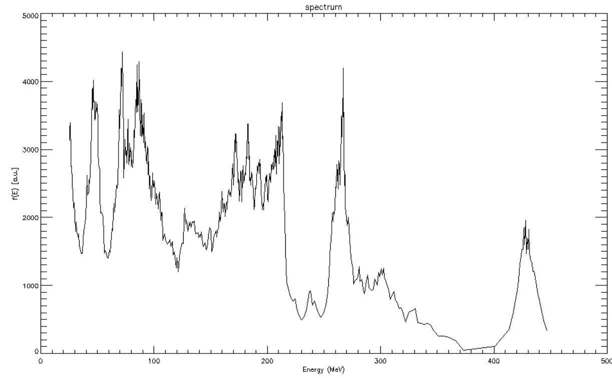

Figure 5: The outgoing spectrum of the injected particles, after the laser has traversed $2.6mm$ of plasma. The peak at $425MeV$ contains $880pC$ of charge, with emittance $\epsilon_x = 2\pi$ mm rad and $\epsilon_y = 25\pi$ mm rad. There is also a monoenergetic peak of $950pC$ in the second bucket (not shown here - visible in Figure 4), at $210MeV$ with emittance $\epsilon_x = 3\pi$ mm rad and $\epsilon_y = 5\pi$ mm rad.

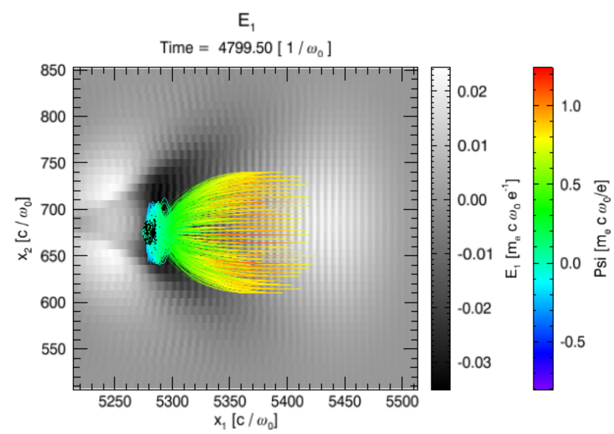

Figure 6: 2D cross-section of the wake superimposed with the tracks of the particles from the ionization-injection run. Notice the particles here are injected nearer the axis then in Figure 3. Although $|\Psi_f|$ is smaller, $\Delta\Psi \approx -1$.

REFERENCES

[1] W. Lu, M. Tzoufras, and C. Joshi, Phys. Rev. STAB. 10 (2007) 061301

[2] T. Tajima and J. M. Dawson, Phys. Rev. Lett. 43 (1979) 267.

[3] P. Chen, J. M. Dawson, Robert W. Huff, and T. Katsouleas, Phys. Rev. Lett. 54 (1985) 693

[4] W. P. Leemans, Nature Phys. 2 (2006) 696

[5] E. Oz, T. Katsouleas, P. Muggli, Phys. Rev. Lett. 98 (2007) 084801

[6] A. Pak, K. A. Marsh, S. F. Martins, W. Lu, W. B. Mori, and C. Joshi, Phys. Rev. Lett. 104 (2010) 025003

[7] W. Lu, Ph.D. Dissertation, UCLA (2006)